Proceedings of ICEGEE 2026 Symposium: Sustainable Environment and Ecology: Supporting a Sustainable Environment for Birds
DOI: 10.54254/2753-8818/2026.BH32745

# *Linking Typhoon Trajectories, Exposure, and Economic Losses: An Impact-Oriented Analysis for Japan*

**Siheng Fei**

*School of Remote Sensing and Information Engineering, Wuhan University, Wuhan, China*
*feisiheng@outlook.com*

***Abstract.*** Tropical cyclones cause significant economic losses in Japan, where high population density and concentrated assets make impacts uneven across regions. This study builds an impact-oriented framework to explain why losses differ between events by linking typhoon tracks, regional exposure, and observed socio-economic losses. Typhoon tracks are classified using a hierarchical, rule-based method that combines simple shape features with spatial contact indicators. A composite loss indicator is constructed from population, housing, and agricultural losses. Event impacts are modeled with a parsimonious hazard–exposure regression using typhoon intensity, land-contact intensity, and a PCA-based exposure index. According to the findings, a different pattern of exposure has been shown to be related to each trajectory type, whereas trajectory/land interaction influences impact analysis. Specifically, the regression shows that the intensity of the typhoons will primarily drive loss on the east-side; however, contact with land and exposure to hazards will have a much less stable and smaller effect on overall loss results. Cross-validation demonstrates that the study's framework provided reasonable and interpretable descriptions of loss differences based on small sample sizes.

***Keywords:*** Typhoon impacts, Trajectory classification, Economic loss assessment, Hazard, Exposure

## 1. Introduction

Tropical cyclones are one of the most destructive natural hazards in East Asia. They often cause significant economic losses. In Japan, many coastal areas have high population density and high concentrations of assets. These regions are therefore highly exposed to typhoon-related hazards. As a result, assessing economic losses caused by typhoons is an essential part of disaster risk management [1].

Methods exist to estimate economic losses attributable to typhoons, including both statistical and machine-learning methods. However, it is difficult to precisely assess losses since the impacts of typhoons depend on several inter-related factors, and to some extent on firm spatial heterogeneity. In Japan, population/asset distributions are heterogeneous, and different typhoon tracks impact different areas leading to very different patterns of impact between otherwise similar events. Finally,

DOI: 10.54254/2753-8818/2026.BH32745

studies use different indicator systems and model structures, which reduces comparability of existing results [2].

From a risk assessment view, economic losses depend on hazard intensity, exposure, and vulnerability. Because typhoons follow different paths and affect other regions, their loss patterns also differ. This study asks how to classify typhoon tracks affecting Japan in an impact-oriented way and whether combining track information with regional exposure can help explain these differences. It provides a more exposure-focused view of typhoon tracks and shows that hazard and exposure together shape economic losses in Japan.

## 2. Literature review

Many studies have examined the impacts and risks of typhoon disasters, and severe events in Japan have caused large economic and social losses, underscoring the need for robust risk assessment frameworks. As a result, existing work has used various statistical and modeling methods, often focusing on rainfall, flooding, and overall damage intensity.

From a methodological perspective, impact assessment primarily follows two paradigms: risk-based approaches that estimate the probability of extreme outcomes, and storyline approaches that describe the evolution of individual events in a physically consistent manner [3].

While other researchers classified typhoon paths based on geometrical features and large-scale steering flows as westward moving, recurving or northward moving types [4], leaving aside the ideas of exposure or space relation with the effects of the storm. More recent studies also note that while "most studies" tend to emphasize overall effects of typhoons, there is comparatively little exploration of the geographic variation in effects along typhoon paths" [5]. Differences in indicators and model structures also reduce comparability and make region-specific analysis more difficult, underscoring the need for frameworks that better capture the spatial heterogeneity of typhoon impacts.

## 3. Methodology

### 3.1. Typhoon trajectory classification

#### 3.1.1. Data collection and preprocessing

This study uses best-track typhoon data from the Japan Meteorological Agency (JMA) for the period 2017–2020. Only effective events, defined as typhoons that approached or made landfall in Japan, are retained to ensure a clear spatial link with the study area. To make different tracks comparable, each trajectory is resampled to a fixed number of points (N = 60), allowing morphological and spatial indicators to be computed on an everyday basis and reducing bias from unequal track lengths or time steps.

#### 3.1.2. Morphological feature extraction

Let a resampled typhoon trajectory in a projected coordinate system be represented as

$$\{(x_i, y_i)\}_{i=1}^{N} \tag{1}$$

The bearing angle between consecutive points is defined as

DOI: 10.54254/2753-8818/2026.BH32745

$$\theta_i = \mathrm{atan2}\,(y_{i+1}\text{-}y_i, x_{i+1}\text{-}x_i),\ \ i=1,\ldots,N\text{-}1, \tag{2}$$

and mapped to the range $[0,360)$.

To characterize turning behavior along the track, the inter-segment turning angle is computed as

$$\Delta\theta_i = \mathrm{wrap}\,(\theta_i\text{-}\theta_{i\text{-}1}) \in (-180,180],\ \ i=2,\ldots,N\text{-}1, \tag{3}$$

the maximum turning angle $T_{max}=\max_i|\Delta\theta_i|$,

the cumulative turning strength $T_{sum}=\sum_i|\Delta\theta_i|$,

and the mean movement direction, calculated using the circular mean,

$$\theta_{mean} = \mathrm{atan2}\left(\frac{1}{m}\sum_i \sin\theta_i, \frac{1}{m}\sum_i \cos\theta_i\right), \tag{4}$$

where $m=N\text{-}1$

These morphological indicators are not used as direct classifiers but serve as structural constraints, ensuring that the geometric characteristics of a track are consistent with its assigned category.

### 3.1.3. Spatial contact feature extraction

To quantify the interaction between typhoon tracks and Japan, spatial contact indicators were constructed using a GIS-based framework. The Japanese mainland geometry is denoted as $\Omega_M$, and an influence buffer is defined as

$$\Omega_g = p \mid d\,(p,\Omega_M) \le D_g, \tag{5}$$

Where $D_g=200$ km.

Let the typhoon track be represented as a polyline $L$. The length of the track within the influence buffer is defined as

$$l_g = \mathrm{len}\,(L \cap \Omega_g), \tag{6}$$

and the overland traversal length is defined as

$$l_{land} = \mathrm{len}\,(L \cap \Omega_M). \tag{7}$$

Figure 1 shows the spatial configuration used to compute influence-buffer and overland contact lengths.

DOI: 10.54254/2753-8818/2026.BH32745

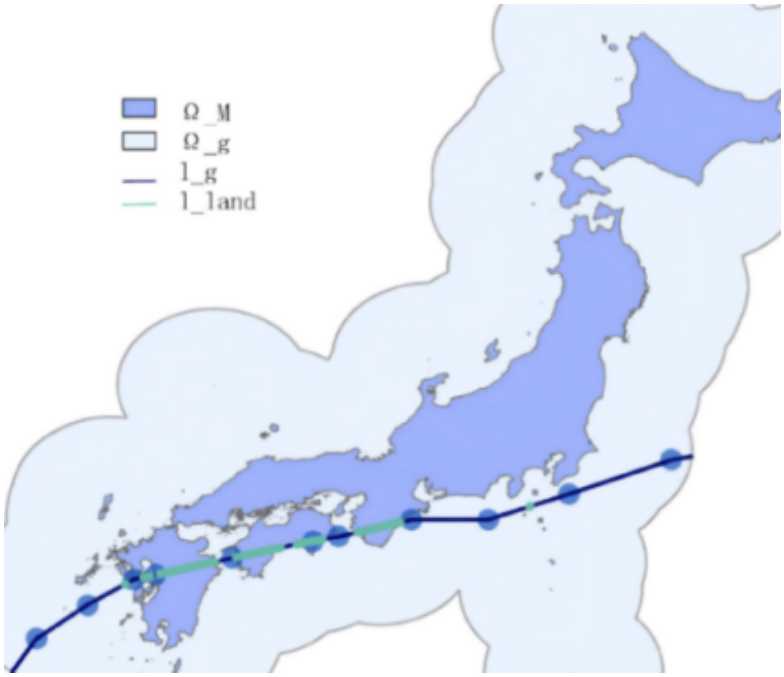


Figure 1. Geometric definition of track–land interaction

### 3.1.4. East–west contact indicators

For track segments located within the influence buffer, the relative position of each trajectory point with respect to the coastline is evaluated. For a point $P$ within $\Omega_g$, its nearest projection point $Q$ on the mainland coastline $\partial\Omega_M$ is identified. The sign of the east–west coordinate difference $(x_P\text{-}x_Q)$ determines whether the point lies on the eastern or western side of the coastline.

Based on this criterion, the east-side and west-side contact proportions are defined as

$$pE=\frac{\#\{P\in P_g:\, x_P\text{-}x_Q>0\}}{|P_g|},\ pW=\frac{\#\{P\in P_g:\, x_P\text{-}x_Q<0\}}{|P_g|}, \tag{8}$$

The two indicators characterize the dominant along-coast interaction pattern of a typhoon.

### 3.1.5. Morphological grouping and hierarchical classification

Trajectory classification is conducted using a hierarchical, rule-based framework with expert review, rather than by parallel threshold comparison. At the top level, trajectories are first grouped into two morphological classes:

- Straight: tracks exhibiting low overall turning and a stable movement direction;
- Recurving: tracks displaying significant directional change.

This top-level grouping provides a structural separation of fundamentally different trajectory geometries.

Only Recurving tracks are further subdivided based on spatial contact characteristics. For these tracks, classification follows a layered decision logic, as illustrated in Figure 2, which presents the hierarchical decision structure based on overland interaction and east–west contact dominance.

DOI: 10.54254/2753-8818/2026.BH32745

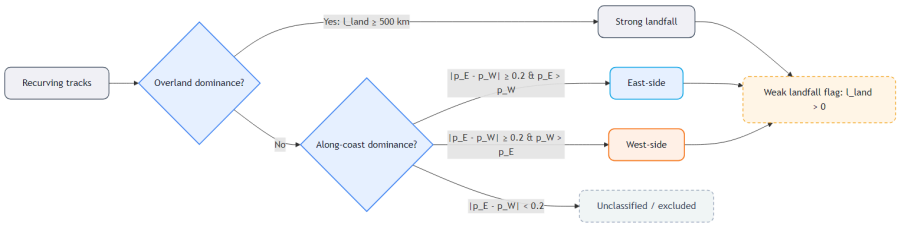


Figure 2. Decision structure for recurving tracks

Tracks with $l_{land} \geq 500$ km km are labeled as strong landfall; otherwise, dominant along-coast contact ( $pE$ and $pW$ ) is used to assign east-side or west-side types, with $l_{land} > 0$ marked as weak landfall, while unstable or mixed cases are excluded.

### 3.1.6. Expert review and quality control

Rather than treating these thresholds as fixed constants JMA track maps are used to adjust them. Borderline events are checked by hand to see if the shape of track matches the spatial contact, while events on the edge or with little real interaction with Japan are dropped. This expert-in-the-loop idea (following a quality-first idea) focuses on meaningful hazard–exposure combinations rather than sample size [6]

## 3.2. Impact modeling framework

### 3.2.1. Modeling philosophy

The modeling strategy adopts an impact-oriented framework. Rather than using a purely meteorological intensity model, it links hazard characteristics, regional exposure, and observed event-level losses. Given the limited number of officially recorded major typhoons and the strong spatial heterogeneity of impacts, the strategy emphasizes interpretability, physical plausibility, and robustness under small-sample conditions. Accordingly, a parsimonious statistical framework is adopted, consistent with impact-based disaster assessment approaches commonly used in recent literature [7].

### 3.2.2. Composite loss indicator $A_0$

Figure 3 presents the structural composition of $A_0$ , showing how population, housing, and agricultural losses are integrated.

DOI: 10.54254/2753-8818/2026.BH32745

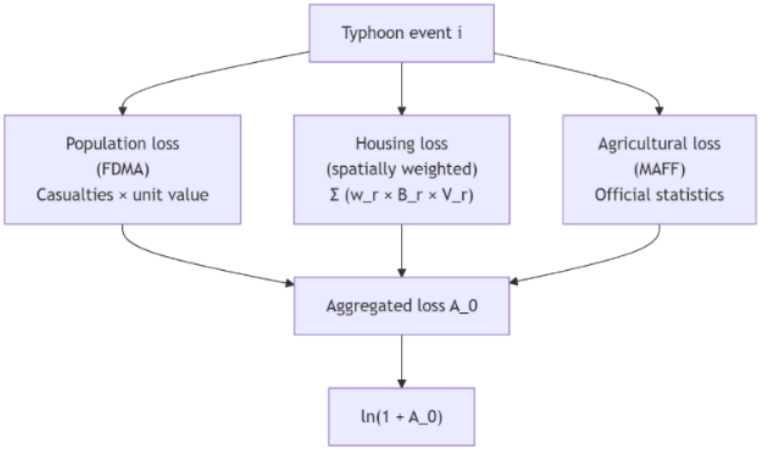


Figure 3. Structure of the composite loss indicator

(1) Conceptual design

The dependent variable $A_0$ is constructed as a composite indicator that integrates multiple impact pathways.

Formally, it consists of three loss-related submodules:

• population-related loss,

• housing-related loss,

• agricultural loss.

Each component is calculated at the event level and subsequently aggregated.

(2) Population-related loss

Population-related loss is derived from casualty and injury statistics reported in the Wind and Flood Damage Reports by the Japanese Fire and Disaster Management Agency (FDMA). For each event, the number of affected individuals is multiplied by an assumed unit compensation value (10 million JPY per person), reflecting disaster relief and insurance practices.

(3) Housing-related loss

Figure 4 illustrates the spatial heterogeneity of baseline housing exposure across Japan, highlighting regional differences in residential density and property values.

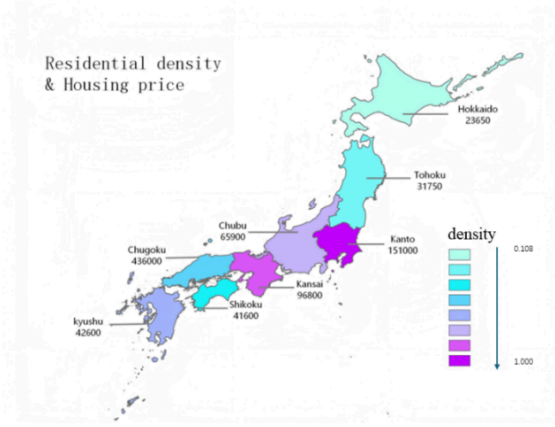


Figure 4. Baseline housing exposure by region

DOI: 10.54254/2753-8818/2026.BH32745

To incorporate the spatial variation, housing loss is modeled using a weighted aggregation structure:

$$L_{house} = \sum_r w_r \cdot B_r \cdot V_r \quad (9)$$

where $w_r$ denotes the regional exposure weight derived from the spatial interaction between the typhoon influence area and region $r$; $B_r$ represents baseline residential exposure (housing density); and $V_r$ denotes representative housing price levels.

A unified assumption on the damaged housing area is adopted to avoid introducing additional free parameters.

(4) Agricultural loss

Agricultural loss is obtained directly from official statistics published by the Ministry of Agriculture, Forestry, and Fisheries of Japan (MAFF), which reflect the damage caused by each typhoon event.

The three components are summed to form $A_0$, and $\ln(1+A_0)$ is used in the regression to reduce skewness and stabilize variance.

### 3.2.3. Exposure indicators $E_1$,$E_2$,$E_3$

Exposure indicators are designed to characterize regional vulnerability and asset concentration, independent of typhoon dynamics [8].

- $E_1$ captures built-environment exposure, primarily reflecting residential asset concentration;
- $E_2$ represents population exposure, serving as a proxy for potential human vulnerability;
- $E_3$ reflects economic or land-value-related exposure, capturing regional differences in asset intensity.

### 3.2.4. Hazard indicators $H_1$,$H_2$,$H_3$

Hazard indicators describe the physical characteristics of typhoon events, incorporating both atmospheric intensity and land interaction [9]:

- $H_1$ : intensity-related indicator (e.g., maximum wind speed);
- $H_2$ : duration-related indicator, reflecting cumulative or sustained influence;
- $H_3$ : land-contact intensity.

Definition of $H_3$ :

The land-contact intensity indicator $H_3$ is constructed based on the overland traversal length of each typhoon track, denoted as $l_{land}$, which is obtained from the trajectory–land interaction analysis. A larger $l_{land}$ indicates deeper and more persistent interaction with the Japanese mainland, and is therefore associated with higher potential for compound impacts.

### 3.2.5. Exposure index construction

$E_{index}$ is not a single exposure variable, but a one-dimensional composite indicator obtained from Principal Component Analysis (PCA), which is a weighted linear combination of the standardized $E_1$, $E_2$, and $E_3$.

Figure 5 shows the loadings of the first principal component, indicating the relative contributions of $E_1$, $E_2$, and $E_3$ to the composite exposure index.

DOI: 10.54254/2753-8818/2026.BH32745

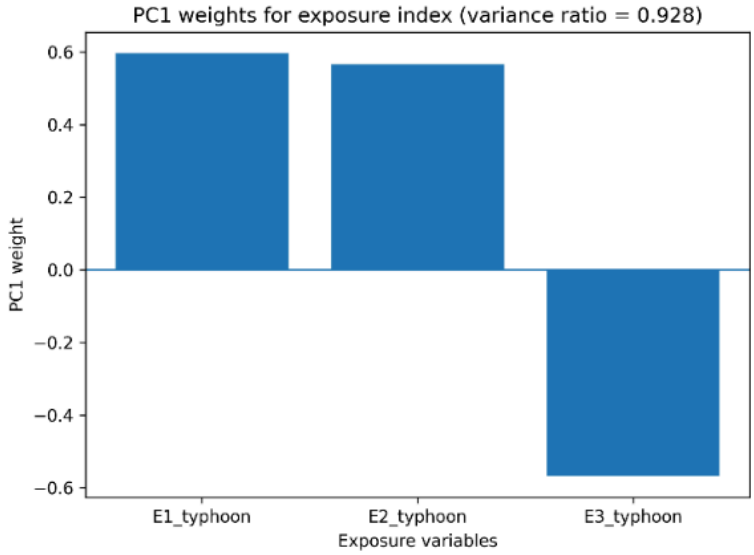


Figure 5. PCA loadings for the exposure index

This step reduces multicollinearity and enhances model stability under small-sample conditions, while preserving the joint information contained in the exposure indicators.

### 3.2.6. Regression model specification

The final regression model relates event-level socio-economic losses to typhoon hazard characteristics and regional exposure conditions. The dependent variable is defined as the logarithmic transformation of the composite loss indicator, $\ln(1+A_0)$ .

Hazard effects are captured by two complementary indicators: $H_1$ , representing typhoon intensity, and $H_3$ , reflecting land-contact intensity derived from overland track traversal. Regional exposure is incorporated through $E_{index}$ .

The regression model is specified as:

$$\ln(1+A_0)=\beta_0+\beta_1 H_1+\beta_2 H_3+\beta 3 E_{index}+\varepsilon.$$

The model is estimated using ordinary least squares (OLS) with heteroskedasticity-consistent HC3 standard errors. Given the limited sample size, leave-one-out cross-validation is further employed to assess model robustness and sensitivity to individual events [10].

### 3.2.7. Modeling scope

This framework is applied to east-side typhoon events as an example of within-type analysis, and it can be extended to the other trajectory types defined above.

## 4. Results

### 4.1. Results of trajectory classification

Based on the hierarchical, rule-based classification framework described in Section 3.1, typhoon trajectories during the study period were categorized into four primary types: east-side, west-side,

DOI: 10.54254/2753-8818/2026.BH32745

landfall-dominant, and straight trajectories. In addition, a small number of events exhibiting mixed spatial contact characteristics were labeled as mix cases for bookkeeping purposes.

Figure 6 shows the proportional distribution of classified trajectory types, with east-side events representing the largest share, followed by landfall-dominant tracks.

Figure 7 shows representative examples of the major trajectory types.

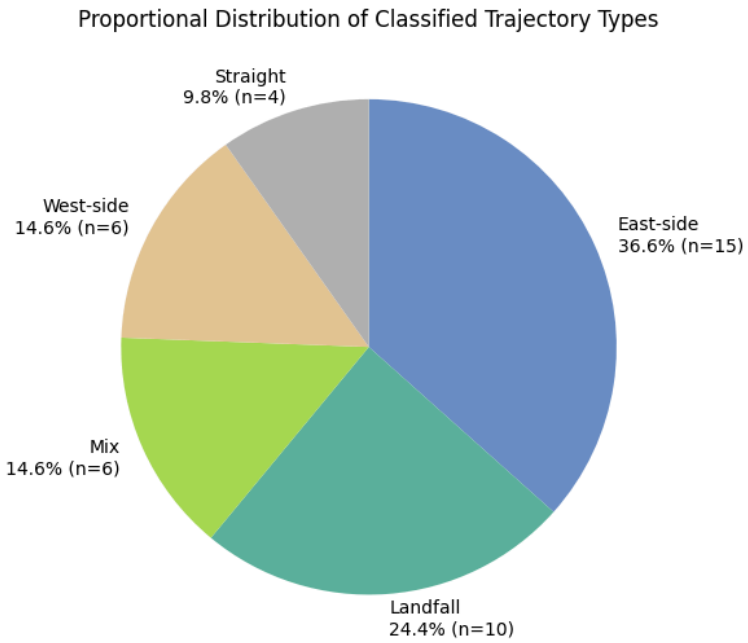


Figure 6. Proportional distribution of classified trajectory types

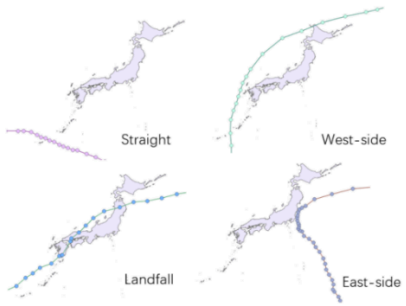


Figure 7. Representative examples of major trajectory types

East-side and west-side trajectories exhibit distinct along-coast interaction patterns relative to the Japanese mainland, whereas landfall-dominant tracks display prolonged overland contact. And straight trajectories generally follow an east-to-west path and mainly affect the Okinawa region.

DOI: 10.54254/2753-8818/2026.BH32745

## 4.2. Exposure characteristics across trajectory types

Figure 8 presents the distribution of the $E_{index}$ across different trajectory types.

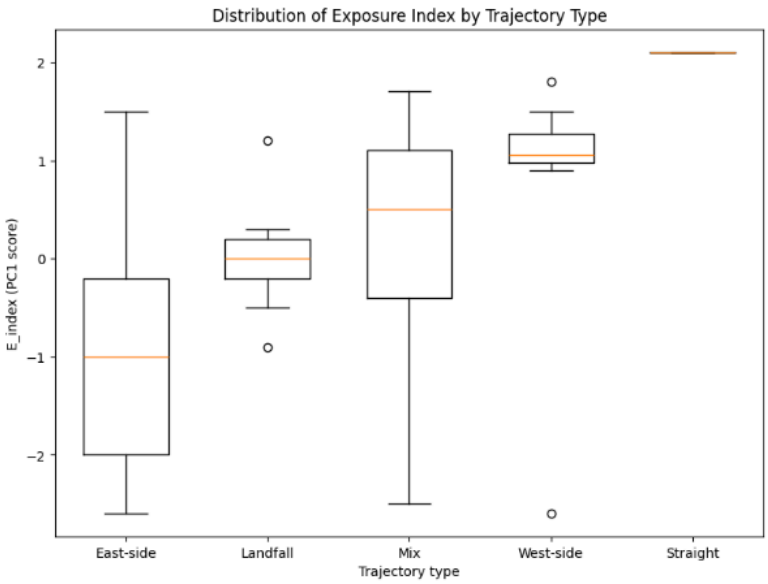


Figure 8. $E_{index}$ by trajectory type

East-side trajectories are associated with lower exposure index values, while west-side and straight trajectories are associated with higher central values. Landfall-dominant events are generally biased towards intermediate exposure levels. Mix cases are the most dispersed, indicating a lack of a strong overall spatial interaction pattern.

The results show that the proposed trajectory classification distinguishes regional exposure patterns, despite some overlap across events. This variability reflects the heterogeneous exposure conditions and supports the subsequent impact modeling.

## 4.3. Regression and robustness results of the impact model

The impact model was applied to the east-side typhoon events. The dependent variable is $\ln(1+A_0)$. Explanatory variables include the normalized intensity indicator ($H_{1\_norm}$), the normalized land-contact indicator ($H_{3\_norm}$), and $E_{index}$ constructed via PCA from three exposure variables ($E_{1\_typhoon}$, $E_{2\_typhoon}$, and $E_{3\_typhoon}$). PCA results show that the first principal component explains 0.928 of the total variance in the standardized exposure variables. Table 1 reports OLS estimates with HC3 heteroskedasticity-consistent standard errors. The final model achieves $R^2 = 0.870$ (adjusted $R^2 = 0.805$).

The estimated regression equation is:

$$\ln(1+A_0) = 12.9680 + 10.6373 \cdot H_{1\_norm} + 3.7986 \cdot H_{3\_norm} - 0.7977 \cdot E_{index}.$$

DOI: 10.54254/2753-8818/2026.BH32745

Table 1. Regression results of the impact model

| Variable | Coefficient | Std. error (HC3) | z | p-value |
|---|---|---|---|---|
| Constant | 12.9680 | 1.606 | 8.074 | 0.000 |
| $H_{1\_norm}$ | 10.6373 | 4.292 | 2.478 | 0.013 |
| $H_{3\_norm}$ | 3.7986 | 4.965 | 0.765 | 0.444 |
| $E_{index}$ | −0.7977 | 1.353 | −0.589 | 0.556 |

Robustness was assessed using leave-one-out cross-validation (LOOCV), yielding MAE = 2.432 and RMSE = 3.022, indicating that the model achieves reasonable, stable explanatory performance in the small-sample setting.

## 5. Conclusion

This study develops an impact-oriented framework to explain typhoon-induced economic losses in Japan by linking trajectory behavior, regional exposure, and observed event-level losses. Typhoon tracks are classified using a hierarchical, rule-based scheme that combines morphological constraints with GIS-based spatial contact indicators, and a composite loss indicator $A_0$ is constructed by integrating population-, housing-, and agricultural losses. Event-level impacts are then modeled using a parsimonious hazard–exposure regression with typhoon intensity, land-contact intensity, and a PCA-based exposure index. The aim is not to build a black-box predictor, but to provide an interpretable explanation of loss differences across events.

The results indicate that the proposed trajectory classification captures systematic differences in exposure conditions, confirming that trajectory–land interaction is a meaningful dimension for impact analysis. For east-side events, typhoon intensity ( $H_1$ ) emerges as the dominant positive driver of losses. In contrast, the effects of land-contact intensity ( $H_3$ ) and the exposure index are weaker and less stable. Model fit and leave-one-out cross-validation suggest that, despite the limited sample size, the framework provides a reasonable and robust explanation of observed loss variations.

Several limitations should be noted. The analysis is restricted to east-side events, the sample size is limited, and the construction of $A_0$ relies on simplifying assumptions. Future work can extend the framework to other trajectory types, incorporate more detailed vulnerability and exposure variables, and develop stratified or type-specific models to capture heterogeneity in typhoon impacts better.

## References

[1] Su, Y. S. (2015). Taiwan vulnerability analysis: a comparative study with Japan, China, USA, UK, France, and the Netherlands. J. Mgmt. & Sustainability, 5, 76.

[2] Liu, X., Liang, Y., Fu, X., Wang, Z., Cai, W., & Zhao, D. (2024, March). Assessment of typhoon disaster loss based on the factor analysis-random forest model. In Journal of Physics: Conference Series (Vol. 2718, No. 1, p. 012043). IOP Publishing.

DOI: 10.54254/2753-8818/2026.BH32745

[3] Tanaka, T., Kawase, H., Imada, Y., Kawai, Y., & Watanabe, S. (2023). Risk-based versus storyline approaches for global warming impact assessment on basin-averaged extreme rainfall: a case study for Typhoon Hagibis in eastern Japan. Environmental Research Letters, 18(5), 054010.
[4] Xu, N., Yang, B., & Ren, J. (2025). Classification of Tropical Cyclone Tracks in the Northwest Pacific Based on the SD-K-Means Model. Applied Sciences, 15(11), 6160.
[5] Wu, D., Huang, M., Zhang, Y., Bhatti, U. A., & Chen, Q. (2018). Strategy for assessment of disaster risk using typhoon hazards modeling based on chlorophyll-a content of seawater. EURASIP Journal on Wireless Communications and Networking, 2018(1), 293.
[6] Jiang, X., Mori, N., Tatano, H., & Yang, L. (2019). Simulation-based exceedance probability curves to assess the economic impact of storm surge inundations due to climate change: a case study in Ise Bay, Japan. sustainability, 11(4), 1090.
[7] Mitheu, F., Stephens, E., Petty, C., Ficchì, A., Tarnavsky, E., & Cornforth, R. (2023). Impact-based Flood early warning for rural livelihoods in Uganda. Weather, climate, and society, 15(3), 525-539.
[8] Raduszynski, T., & Numada, M. (2023). Measure and spatial identification of social vulnerability, exposure and risk to natural hazards in Japan using open data. Scientific reports, 13(1), 664.
[9] Zhang, J., Yan, J., & Li, X. (2024). Study on the impact of population and economic activities on environmental indicators through PCA. Transactions on Economics, Business and Management Research. h t t p s: //d o i. o r g/1 0, 6(2), 0.
[10] Lv, L., Song, X., & Sun, W. (2020). Modify leave-one-out cross validation by moving validation samples around random normal distributions: move-one-away cross validation. Applied Sciences, 10(7), 2448.